COMMUNICATION

Check for updates

Inherent enantioselective adsorption and photocatalytic removal of L-phenylalanine on cerium phosphate films†

Nitai Arbell, [ID] ‡[ab] Shoval Gilboa‡[b] and Yaron Paz [ID] *[ab]

Chiral-surface interactions are of immense importance in the field of enantioseparation, as a way of obtaining chirally-pure compounds. Films of both rhabdophane and monazite-phase cerium phosphate in a silica binder were found to exhibit enantioselective adsorption of the chiral amino acid phenylalanine, purifying racemic solutions to 100% of the D-enantiomer. Likewise, using the photocatalytic properties of cerium phosphate led to enriching racemic mixtures to a D−L ratio of 9:1.

Chemical chirality is a seemingly minor aspect of molecular structure, with surprisingly important implications, especially in the biological world. Biological building blocks, from sugars to nucleic acids and amino acids, are all chiral, and found in nature almost exclusively with a specific handedness. Homochirality has major consequences on the interactions between chiral species and biological systems, leading to different (and oftentimes dramatically so) biological effects of opposite enantiomers of pharmaceuticals, fragrances, pesticides, and so on.[1,2] Despite the inherent need for chirally-pure compounds, enantioseparation remains quite a challenge in modern chemistry, as both enantiomers typically, but not always,[3] display virtually identical physicochemical properties, apart from their interactions with chiral environments. Several approaches towards enantiopurity have been developed, including the asymmetric synthesis of enantiopure products,[4] or the separation of racemic mixtures, for example, through chiral chromatography.[5] However, there is still a technological gap requiring bridging for the robust and economical enantiopure production of many compounds.[6,7] Asymmetric spatial interactions, which are at the base of most

of these separation methods, may take on several different forms. Here, the structure of the moiety with which the chiral specie interacts (*e.g.* crown ethers, diastereomeric salt-forming auxiliaries) is critically important.[8] Chiral selectivity also exists for surface-adsorbate interactions, due to chirality-inducing differences in the micro- or macrostructure of the surface.[9–13] It is not always fully clear, however, what the source of this preference is, which can also further manifest in phenomena such as different electrochemical signals upon the interaction of different enantiomers with an achiral electrode.[4,14]

One enantio-separation method that has shown promise in recent years is enantioselective photocatalysis, which allows kinetic resolution of racemic mixtures by the preferential degradation of one enantiomer in a mixture, leaving its counterpart intact. This preference can be induced by molecular imprinting of the target enantiomer to be degraded in the photocatalytic matrix, resulting in its preferential adsorption and photodegradation,[15] or by the inclusion of chiral templates for the growth of chiral photocatalytic structures.[16,17] The work discussed here, however, describes an inherent chiral selectivity, resulting in enantio-resolution of mixtures of L- and D-phenylalanine (PA), in hybrid CePO$_4$–SiO$_2$ films, without the addition of any chiral modifiers. This inherent enantioselectivity effect was noted in CePO$_4$ both for adsorption under dark conditions, and for photocatalytic reactions, but was not displayed at all by similar films of TiO$_2$, a benchmark photocatalyst. This work has the potential to expand the range and applicability of enantioselective heterogenous interactions as a chiral separation method, based on both adsorption and photocatalytic modes. Additionally, this research has possible implications on the asymmetric origins of life,[18] with CePO$_4$ known to be a catalyst capable of the formation of nucleotides and other biomolecules.[19]

Catalyst films were deposited by spin-coating on glass slides. Three types of films were tested: a commercial, rhabdophane-phase, cerium phosphate, a synthesized, monazite-phase, cerium phosphate (both used as is), and P25 titania, all in a silica binder. Characterization was carried out by XRD, scanning electron microscopy, energy dispersive X-ray spectroscopy (SEM-EDS) and

[a] The Russell Berrie Nanotechnology Institute, Technion-Israel Institute of Technology, Haifa 3200003, Israel. E-mail: Paz@technion.ac.il

[b] The Wolfson Department of Chemical Engineering, Technion-Israel Institute of Technology, Haifa 3200003, Israel

circular dichroism (CD). The films were placed in a Radley's carousel parallel reaction system with racemic and enantiopure solutions of L- and D-phenylalanine (PA), and either left for 48 hours in the dark under stirring, or, following adsorption in the dark for 24 hours, exposed to 365 nm LED illumination for 150 hours. The concentrations of both enantiomers in the reaction solution were monitored using chiral high-performance liquid chromatography (HPLC). Further experimental details can be found in the ESI.†

Fig. S1 and S2 (ESI†) present micrographs and elemental distribution maps of a film of rhabdophane and monazite-phase $CePO_4$ in a silica binder, respectively, used in this work. The figures reveal an even distribution of photocatalytic particles in the silica matrix. P25 films were similarly well-dispersed, as shown in the Fig. S3 (ESI†).

Adsorption and photocatalytic reaction experiments were performed both in enantiopure solutions, containing only L- or D-PA in each reaction vial, as well as in racemic mixtures. Presented in Fig. 1 are exemplary chromatograms for racemic mixtures before (Fig. 1A) and after 48 hours of adsorption. Similar chromatograms, showing the single-enantiomer adsorption experiments, as well as both racemic and single-enantiomer photocatalytic experiments, are shown in the ESI.† The trends seen in these chromatograms, showing limited uptake of either enantiomer for P25 (Fig. 1B), *versus* a highly selective and complete (or almost so) adsorption of L-PA for both $CePO_4$ phases (Fig. 1C and D), were repeated in duplicates for each film type.

Fig. 2 shows exemplary concentration curves, as deduced from the HPLC analysis, for the adsorption experiments. In all measured samples, both $CePO_4$ phases (Fig. 2B1, B2, C1 and C2) showed a high adsorption capacity, and a significant selectivity towards the adsorption of L-PA. Single-enantiomer experiments (Fig. 2B1 and C1) showed the same trend, *i.e.*, preferential adsorption of L-PA. Here, the selectivity ratio was higher (since

no adsorption of D-PA was measured), however, the adsorptivity was somewhat lower. The faster adsorption in the racemic experiments is intriguing and in contrast to our experience in imprinting-induced chiral separation.[15] A possible explanation could be the inclusion of D-PA within the growing multilayers, that assists in overcoming nascent mismatch faults. At any case, this issue is still under study. In contrast to $CePO_4$-containing films, no enantioselective adsorption was observed on both P25 films containing silica binder (Fig. 2A1 and A2) and on films made of pristine silica binder (Fig. S13, ESI†).

An important observation that was noted in all $CePO_4$ films was the presence of a lag-time in the adsorption of L-PA, suggesting a mechanism requiring the formation of an initial nucleation site before the more rapid adsorption of consequent layers.

Fig. 3 presents exemplary concentration curves for the photocatalytic experiments, split into two regions, with negative times denoting the (dark) period of adsorption on the films, before the start of illumination at $t = 0$. Control experiments showed no appreciable photolysis or dark hydrolysis under reaction conditions without a catalyst (ESI†). In a similar manner to the adsorption reactions, while films of both $CePO_4$ phases showed significantly enhanced selectivity towards the removal of L-PA, in both racemic and single enantiomers experiments (Fig. 3B1, B2, C1 and C2), films comprising of titania P25 and silica binder showed no enantioselectivity (Fig. 3A1 and A2). Unlike the adsorption reaction, in enantiopure solutions (Fig. 3A1, B1 and C1), complete removal was achieved after 150 hours (for both enantiomers in the case of P25, only for L-PA in both phases of $CePO_4$), yet, for racemic solutions, a much lower reaction rate was observed.

A potential explanation for the fact that the reaction rates with the racemic solutions were lower than those with the single enantiomers could be the higher concentration in the single enantiomer experiments relative to the racemic mixture experiments.

Comparing the kinetic data presented in Fig. 2 and 3, it is evident that the disappearance of PA from the liquid phase was faster in the adsorption experiments than in the photocatalytic experiments, in which both adsorption and photocatalysis contribute. Moreover, carrying out adsorption under dark conditions appears to better and faster separate L-PA from D-PA than performing adsorption and photocatalysis under illumination. These findings are seemingly counterintuitive. Since a negligible temperature rise was measured in the reaction vessels during illumination, a likely explanation could be the photocatalytic removal of L-PA from the surface, inhibiting its nucleation, a necessary stage for selective adsorption. This stage is rather slow, as is evident by the observation of lag-time (Fig. 2). This explanation is corroborated by the apparent 1st order kinetics (ESI†), which is different from the apparent zero order kinetics reported in the photocatalytic degradation of multilayers.[20]

The end-results from both types of experiments in racemic solutions were averaged over all repetitions (up to 6). All repetitions showed the same trend. Fig. 4A and B present the percentage of overall removal of each enantiomer from the racemic mixtures during adsorption and photocatalysis,
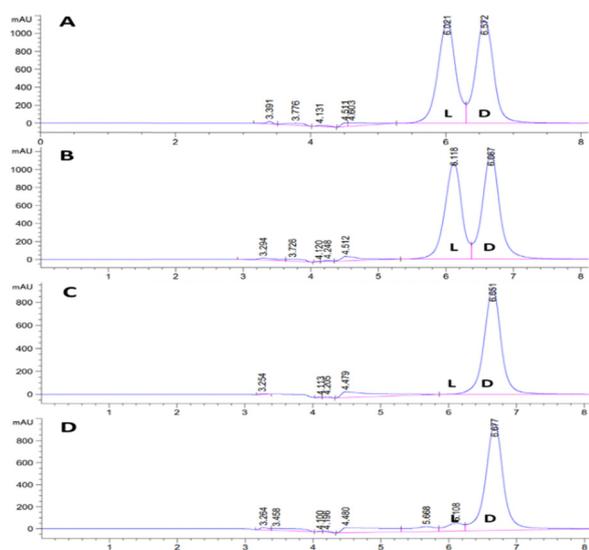

Fig. 1 Chiral HPLC chromatograms of phenylalanine (A) before reaction, and (B)–(D) after 48 hours of adsorption under dark conditions on (B) P25, (C) rhabdophane $CePO_4$ and (D) monazite $CePO_4$ films.
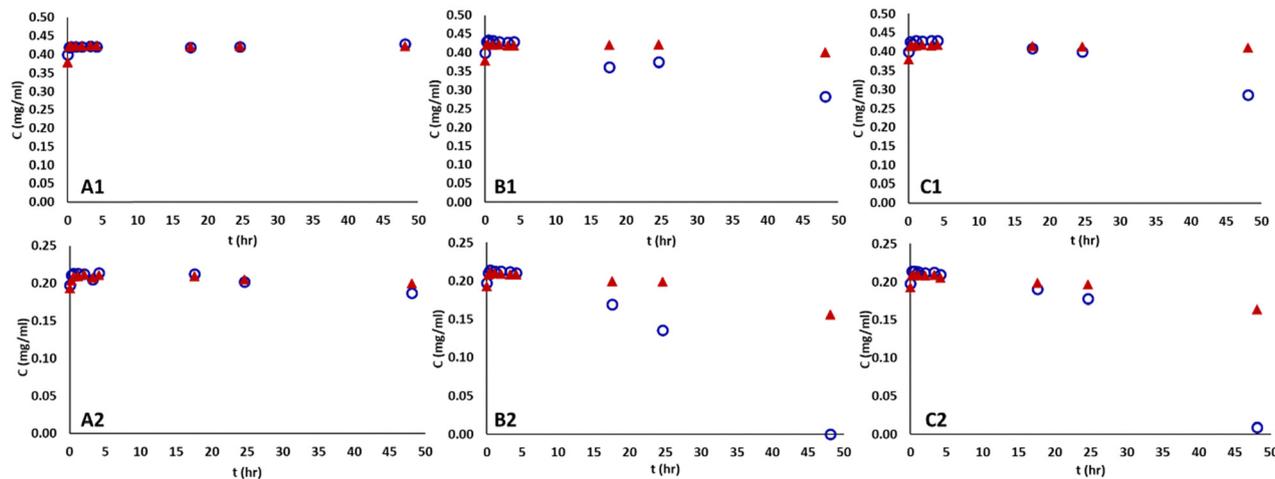
Fig. 2 Exemplary concentration curves for the adsorption under dark conditions of L- (blue circles) and D-phenylalanine (red triangles), as measured in solution for (A) P25, (B) rhabdophane CePO₄ and (C) monazite CePO₄ films, for (1) a single enantiomer at a time, and (2) racemic mixtures.
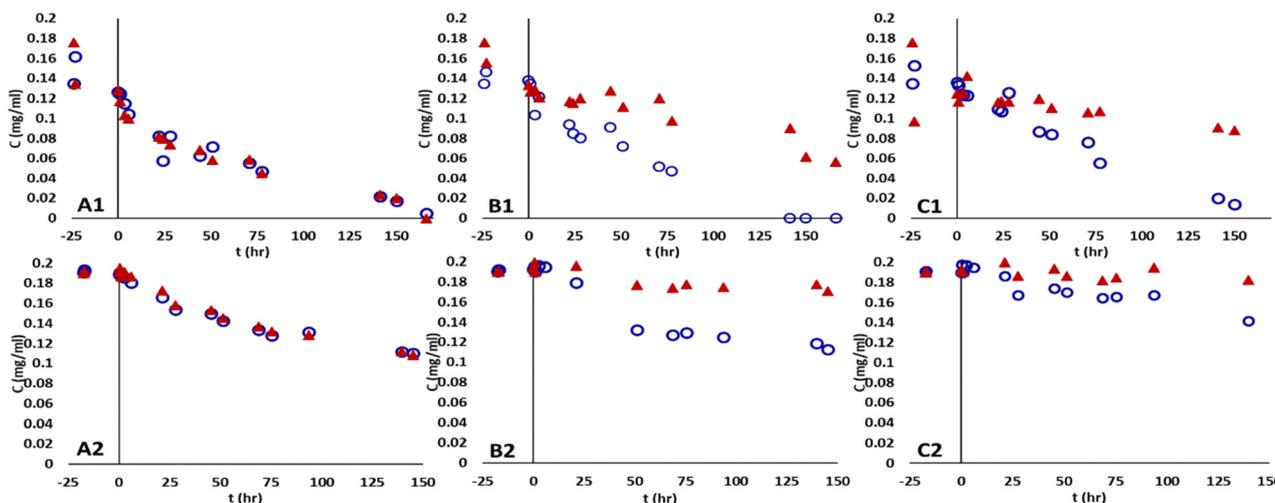

Fig. 3 Exemplary concentration curves for the photocatalytic reaction of L- (blue circles) and D-phenylalanine (red triangles), as measured in solution for (A) P25, (B) rhabdophane CePO₄ and (C) monazite CePO₄ films, for (1) a single enantiomer at a time, and (2) racemic mixtures. Negative times denote adsorption under dark conditions before the start of illumination at $t = 0$.

respectively, manifesting the higher removal of L-PA. The photocatalytic selectivity is given in Fig. 4C, presenting the ratio between the apparent first order rate constants (k_L and k_D for L- and D-PA, respectively). This kinetic model showed a good fit for the photocatalytic reactions (ESI†), unlike the adsorption reactions, which present seemingly autocatalytic kinetics. Unlike cerium phosphate, in which this ratio was 5–7 depending on its phase, the obtained ratio with titanium dioxide was 1, as could be expected from a non-selective photocatalyst.

In conclusion, this manuscript shows, for the first time to our knowledge, the capabilities of cerium phosphate as a material exhibiting inherent enantioselectivity towards an amino acid substrate, both as an adsorbing matrix and as a photocatalyst. The enantioselective adsorption on the CePO₄ films was able to completely enrich initially racemic mixtures up to 100% of a single enantiomer, while adsorbing a mixture of around 80% purity of its counterpart. Photocatalytic reactions similarly enriched racemic mixtures, albeit to a lower extent, and over significantly longer time periods.

Additional preliminary work on a chemically different amino acid, citrulline, showed the same effect (ESI†), suggesting that this reported phenomenon may be general. It is possible, yet still not proved, that this reported enantio-selectivity is connected to the fact that rhabdophane has the chiral Söhncke space group symmetry of $P3_121$–$P3_221$,[21] and that monazite has a $P2_1$ symmetry, which, although not considered an enantiomorphic space-group, still forms a chiral superstructure.[18,22,23] Indeed, a similar effect of selective adsorption on an inherently chiral surface (L-serine on (CrMoTa)Si₂ having a C40 P6₂22 crystal structure) was reported recently.[24]
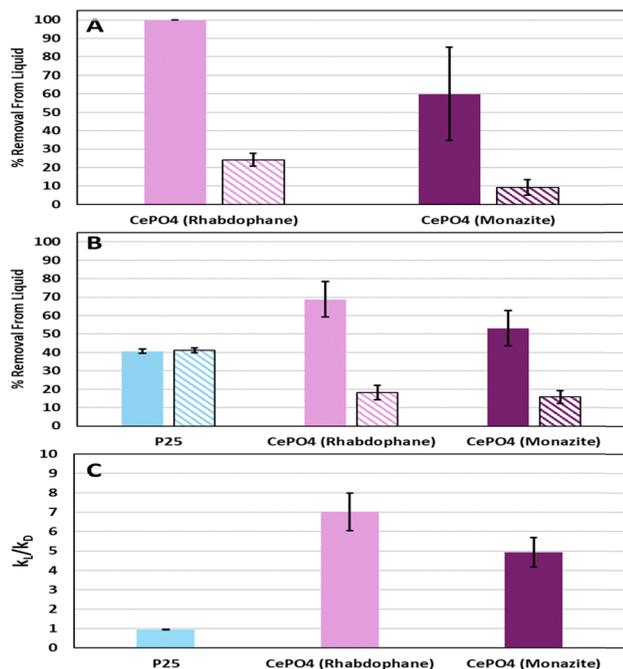
Fig. 4 Averaged percent removal of L-PA (full bars) and D-PA (striped bars) from the liquid phase following adsorption in the dark (A) and following photocatalytic reaction (B). The averaged enantiospecific kinetic constant ratio (k_L/k_D) in the photocatalytic reactions is also given (C).

In an attempt to gain insight on the origin of the enantios-electivity of cerium phosphate, circular dichroism measurements were performed on the $CePO_4$ particles embedded in KBr pellets, according to an established technique.[25] Unfortunately, results were inconclusive, although some dichroic signal was observed (ESI†). Likewise, EBSD-SEM and polarimetry did not yield any meaningful information due to the small size of the crystallites and scattering effects, respectively. We would like to emphasize that enantioselective adsorption is not limited to chiral crystals but may appear on non-chiral crystals exposing chiral surfaces.[13] All in all, the origin of the enantio-selectivity of cerium phosphate is still under investigation by us, in particular in the context of origin of life.

While it is evident that in this specific case, enantioselective adsorption is a markedly efficient chiral purification method, the fact that the enantio-selectivity of the surface interactions is carried over to the photocatalytic reaction may be useful in different reaction systems or applications. Moreover, due to the theorized importance of both silicate minerals[18] and $CePO_4$ in the origin of life,[19] these findings may even have implications on our understanding of the origin of homochirality in biological systems. Additional investigations into the matter will be published in a follow-up article.

All authors contributed significantly to the work presented in this manuscript. S. Gilboa and N. Arbell carried out all aspects of this research equally, under the guidance of Y. Paz.

Conflicts of interest

There are no conflicts to declare.

Data availability

The data supporting this article have been included as part of the ESI.†

References

1 G. H. Wagnière, *On Chirality and the Universal Asymmetry*, Verlag Helvetica Chimica Acta, Zürich, 2007.
2 L. Nguyen, H. He and C. Pham-Huy, *Int. J. Biomed. Sci.*, 2006, **2**, 85–100.
3 M. Ebrahimi, P. Norouzi, J. B. Ghasemi, A. A. Moosavi Movahedi, M. Noroozifar and R. Salahandish, *Sci. Rep.*, 2023, **13**, 16739.
4 R. Noyori, S. Hashiguchi and T. Yamano, Asymmetric Synthesis, *Applied Homogeneous Catalysis with Organometallic Compounds*, ed., B. Cornils, W. A. Hermann, Wiley-VCH, Weinheim, 3rd edn, 2002, pp. 557–584.
5 S. Al-Sulaimi, R. Kushwah, M. A. Alsibani, A. El Jery, M. Aldrdery and G. A. Ashraf, *Molecules*, 2023, **28**, 6175.
6 J. Sui, N. Wang, J. Wang, X. Huang, T. Wang, L. Zhou and H. Hao, *Chem. Sci.*, 2023, **14**, 11955–12003.
7 F. Malacarne, S. Grecchi, M. Niamlaem, B. Bonczak, G. Salinas and S. Arnaboldi, *Anal. Bioanal. Chem.*, 2024, **416**, 3677–3685.
8 G. K. E. Scriba, *J. Chromatogr. A*, 2016, **1467**, 56–78.
9 Y. Yun and A. J. Gellman, *Angew. Chem., Int. Ed.*, 2013, **52**, 3394–3397.
10 T. Serizawa, T. Sawada and M. Wada, *Chem. Commun.*, 2013, **49**, 8827–8829.
11 A. S. Daniels, A. J. Gellman and E. C. H. Sykes, *Chem. Commun.*, 2024, **60**, 8383–8386.
12 S. Arnaboldi, M. Magni and P. R. Mussini, *Curr. Opin. Electrochem.*, 2018, **8**, 60–72.
13 F. Zaera, *Chem. Soc. Rev.*, 2017, **46**, 7374.
14 M. Forester and R. Raval, *Chem. Commun.*, 2016, **52**, 14075–14084.
15 N. Arbell, K. Bauer and Y. Paz, *ACS Appl. Mater. Interfaces*, 2021, **13**, 39781–39790.
16 X. Yue, L. Xu, H. Lin, C. Xu and S. Li, *Sci. Bull.*, 2023, **68**, 1764–1771.
17 S. Li, M. Veksler, Z. Xu, L. Xu, C. Xu and N. A. Kotov, *ACS Energy Lett.*, 2021, **6**, 1405–1412.
18 C. Lee, J. M. Weber, L. E. Rodriguez, R. Y. Sheppard, L. M. Barge, E. L. Berger and A. S. Burton, *Symmetry*, 2022, **14**, 460.
19 S. Gilboa, L. Panz, N. Arbell and Y. Paz, *Life*, 2024, **14**, 846.
20 Y. Paz, Z. Luo, L. Rabenberg and A. Heller, *J. Mater. Res.*, 1995, **10**, 2842–2848.
21 D. Avnir, *Minerals*, 2024, **14**, 995.
22 H. D. Flack, *Helv. Chim. Acta*, 2003, **86**, 905–921.
23 M. Miyata, N. Tohnai, I. Hisaki and T. Sasaki, *Symmetry*, 2015, **7**, 1914–1928.
24 C. Chen, Y. Ma, K. Yao, Q. Ji and W. Liu, *Nat. Commun.*, 2024, **15**, 10105.
25 I. Azumaya, I. Okamoto, S. Nakayama, A. Tanatani, K. Yamaguchi, K. Shudo and H. Kagechika, *Tetrahedron*, 1999, **55**, 11237–11246.